EUROFUSION WPJET1-PR(16) 15708

L Braiden et al.

Transition to turbulence in Hunt's flow in a moderate magnetic field

Preprint of Paper to be submitted for publication in
Journal of Fluid Mechanics

This work has been carried out within the framework of the EUROfusion Consortium and has received funding from the Euratom research and training programme 2014-2018 under grant agreement No 633053. The views and opinions expressed herein do not necessarily reflect those of the European Commission.

Transition to turbulence in Hunt's flow in a moderate magnetic field

L. Braiden[1]†, D. Krasnov[2], S. Molokov[1], T. Boeck[2] and L. Bühler[3]

[1]School of Computing, Electronics and Mathematics, Coventry University, Priory Street, Coventry CV1 5FB, UK

[2]Institute of Thermodynamics and Fluid Mechanics, Technische Universität Ilmenau, 98684 Ilmenau, Germany

[3]Institut für Kern- und Energietechnik, Karlsruher Institut für Technologie, 76021 Karlsruhe, Germany

(Received xx; revised xx; accepted xx)

Pressure-driven magnetohydrodynamic duct flow in a transverse uniform magnetic field is studied by direct numerical simulation. The electric boundary conditions correspond to Hunt's flow with perfectly insulating walls parallel to the magnetic field (side walls) and perfectly conducting walls perpendicular to the magnetic field (Hartmann walls). The velocity distribution forms strong jets at the side walls, which are susceptible to instability even at low Reynolds numbers Re. We explore the onset of time-dependent flow and transition to fully-developed turbulent states for a moderate Hartmann number $Ha = 100$. At low Re time-dependence appears in the form of elongated Ting-Walker vortices at the side walls of the duct, which, upon increasing Re, develop into more complex structures with higher energy and then the side-wall jets partially detach from the walls. At high values of Re jet detachments disappear and the flow consists of two turbulent jets and nearly laminar core. It is also demonstrated that, there is a range of Re, where Hunt's flow exhibits a pronounced hysteresis behavior, so that different unsteady states can be observed for the same flow parameters. In this range multiple states may develop and co-exist, depending on the initial conditions.

1. Introduction

Magnetohydrodynamic (MHD) flows in ducts play a major role in liquid metal blankets for thermonuclear fusion reactors serving for cooling of the reactor and for breeding tritium (Bühler 2007). A very important requirement to these flows is that they should provide sufficient mixing of the fluid to improve heat and mass transfer characteristics, i.e. provide sufficient level of turbulence. This, however, may be problematic as the liquid metal flow occurs in a high magnetic field of about $5-10$ Tesla. This leads to high MHD interaction between the induced currents $\mathbf{j}$ and the magnetic field $\mathbf{B}$ resulting in a strong braking Lorentz body force $\mathbf{j} \times \mathbf{B}$, which tends to damp turbulence.

More often than not the ducts have thin electrically conducting walls, which leads to a very unusual velocity profile, shown in Fig. 1. Here the basic velocity exhibits a flat core, exponential Hartmann layers at the walls transverse to the magnetic field (the Hartmann walls), and jets at the walls parallel to the field (the side walls). Jets appear due to induced electric current within the core of the flow. The current must turn (either fully or partially) in the direction of the magnetic field at the side walls to complete the loops, which then close through the conducting Hartmann walls (Fig. 1). Once this

† Email address for correspondence: braidenl@uni.coventry.ac.uk

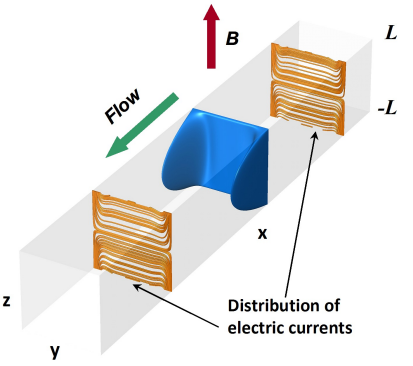

FIGURE 1. Flow geometry of Hunt's flow in a square duct. Laminar velocity distribution with perfectly conducting Hartmann- and perfectly insulating parallel-walls is shown at $Ha = 100$ (blue); also shown are the streamlines of electric current density (brown).

happens, the resulting force $\mathbf{j} \times \mathbf{B}$ and its braking effect are reduced in the near-wall region, thus allowing the fluid to flow with higher velocity than that in the core. The exact ratio of the core to jet velocities and thus between the mass fluxes strongly depends on the electrical conductivities of the Hartmann- and side-walls. In the extreme case of perfectly electrically insulating side walls and perfectly conducting Hartmann walls (known as Hunt's flow, see a particular case in Hunt (1965)), practically all the mass flux is carried by the side-wall jets.

We will be concerned here with an electrically conducting, incompressible fluid flow in a sqaure duct, driven by a constant pressure gradient, with kinematic viscosity, ν, density, ρ, and electrical conductivity, σ. The flow is subjected to a uniform magnetic field of intensity $\boldsymbol{B}$ applied in the z-direction (x, y, z are Cartesian coordinates, as shown in Fig. 1). For a given mean velocity U, the flow is characterised by three dimensionless parameters (Müller & Bühler 2001): the Reynolds number, $Re = UL/\nu$, where L is half the distance between the walls, the Hartmann number $Ha = \boldsymbol{B}L(\sigma/\rho\nu)^{1/2}$, the square of which characterises the ratio between the Lorentz and viscous forces, and the wall conductance ratio $c = \sigma_w h_w/\sigma a$, where σ_w and h_w are the electrical conductivity and thickness of the wall, respectively. Note that c may be different for each wall or pairs of walls.

A family of the exact solutions for MHD flows with jets was obtained by Hunt (1965). Early experimental results were reviewed by Lielausis (1975), and the main conclusion of the authors was that the jets were much thicker than the $O(Ha^{-1/2})$ thickness of the jets in the fully developed flow. Linear stability of a flow in a duct with $c = 0.07$ (Ting *et al.* 1991) could not account for this increase in the thickness as the instability was fully contained in the parallel layers. In addition, the Ting and Walker (TW) vortices appeared for critical Reynolds number $Re_{cr} \sim 300$, while in the corresponding experiment by Reed & Picologlou (1989) the instabilities appeared at $Re_{cr} \sim 3000$. For Hunt's flow linear stability analysis was performed by Priede *et al.* (2010), who discovered a rich variety of perturbations, including streaks for $Ha < 45$, while for higher Ha the most unstable mode consisted of TW vortices. The controvercies between the theory and the experiment were resolved by Knaepen *et al.* (2009); Kinet *et al.* (2009), who for $Ha = 200$ and $c = 0.2$ performed direct numerical simulation (DNS) of the transition to turbulence. First, they have shown that, when TW vortices appear, they are so weak that they do not affect the mean velocity profile. For $Re > 3500$ a new effect appeared consisting of partial jet detachment from the side walls, which indeed led to thicker jets.

In this work we will focus on the transition to turbulence in Hunt's flow and show that

the transition is far more complex and interesting than initially discovered effects, which lead to jet detachment demonstrated by Kinet *et al.* (2009).

2. Procedure and parameters

We consider the incompressible Navier-Stockes equations with an additional Lorentz force term, assuming the limit of a low magnetic Reynolds number Re_m. In this case the so-called quasi-static approximation (Roberts 1967) can be applied and the Lorentz force is represented as $\boldsymbol{F} = \boldsymbol{j} \times \boldsymbol{B}$, where the induced electric current density $\boldsymbol{j}$ is given by Ohm's law $\boldsymbol{j} = \sigma\left(-\nabla\phi + \boldsymbol{v} \times \boldsymbol{B}\right)$. Here $\boldsymbol{v}$ is the velocity vector, σ the electrical conductivity and ϕ the induced electric potential. Neglecting displacement currents and assuming an electrically neutral fluid, the current density $\boldsymbol{j}$ should satisfy the divergence-free constraint $\nabla \cdot \boldsymbol{j} = 0$ resulting in the Poisson equation for the electric potential $\nabla^2\phi = \nabla \cdot (\boldsymbol{v} \times \boldsymbol{B})$.

The governing Navier-Stokes equations with the additional Lorentz body force are solved numerically with our in-house solver (Krasnov *et al.* 2011). The numerical model is based on the 2^{nd} order nearly conservative (for the mass, momentum, electric charge and kinetic energy) finite-difference scheme with collocated grid arrangement. The incompressibility of the velocity field $\nabla \cdot \boldsymbol{v} = 0$ is fulfilled through a projection-correction procedure, which amounts to the solution of a Poisson problem for the pressure field p. The boundary conditions are periodic in the streamwise x-direction. In the wall-normal y- and z-directions the velocity at duct walls has zero slip conditions $\boldsymbol{v} = 0$. For the electric potential these are Neumann type $\frac{\partial\phi}{\partial n} = 0$ at perfectly insulating walls $y = \pm L$ and Dirichlet type $\phi = const.$ at perfectly conducting walls $z = \pm L$.

Time integration has initially been implemented using the fully explicit 2^{nd} order Adams-Bashforth/Backward-differencing scheme. Specially for this study the scheme has been modified for the implicit treatment of the viscous terms $\frac{1}{Re}\nabla^2\boldsymbol{v}$. The semi-implicit version is beneficial at low-Re, as it helps to maintain large integration time-steps δt without the loss of numerical stability. The code is parallelized with hybrid approach (both MPI and Open MP) for the effective use on massive-parallel supercomputers. Further details on the solver, e.g., exact equations, discretization, solution of elliptic problems can be found in Krasnov *et al.* (2011).

The simulations have been conducted on a domain size of $8\pi \times 2 \times 2$ and numerical resolution varied from 512×128^2 to 1024×256^2 points in, correspondingly, x-, y- and z-directions. As we progress further, it will be shown that a relatively long domain becomes essential when the flow develops streamwise-elongated structures upon increasing Re. The computational grid is clustered in the wall-normal y- and z-directions by applying the coordinate transformation based on hyperbolic tangent, e.g., $z = L\frac{\tanh(A\zeta)}{\tanh(A)}$, where $-1 < \zeta < 1$ is the uniform coordinate and A is the strength of clustering. In our simulations we have used $A_y = A_z = 2.5$ in both wall-normal directions to accuratley resolve the region of the side wall jets, where most of the flow dynamics and instability occur.

A series of DNS has been performed at a fixed Hartmann number $Ha = 100$, representing the case of moderate magnetic fields, and a broad range of Re, covering regimes from $Re = 200$ to 10000. A similar approach with fixed Ha and varying Re was also used in a prior study (Kinet *et al.* 2009). In various studies on flow transition the most commonly used scenario is to modulate initially laminar flow by perturbations. For example, these can be either $3D$ random noise of a certain amplitude (one step scenario) or a combination of the so-called optimal perturbations modulated by random noise (two step scenario, e.g., Schmid & Henningson (2001)). In either case the transient evolution and the actual

thresholds are governed by many parameters, including the amplitude of perturbations, specific spatial shape and distribution, optimal wave-numbers, etc.

Therefore, to avoid this ambiguity, two other scenarios of obtaining time-dependent MHD solutions have been adopted. First, we have used fully developed non-MHD turbulent flows precomputed for the closest possible Re number as the initial state. Then the magnetic field is switched on and the simulation is continued further. This method has the appeal that fluctuations are created in a natural way. In another procedure the unsteady MHD solution, obtained for a certain Re, is used as initial state to study evolution to a different target Re, which can be either higher or lower than the initial Re. This method has been most extensively used to study the phenomenon of hysteresis. We have employed both ways of changing Re – with small steps and as a single shot to the target value. The onset of new unsteady solutions or transition between different states have been identified by visual analysis of the flow field and by monitoring the kinetic energy of the transverse velocity components $q_t = u_y^2 + u_z^2$. This quantity has been confirmed as a robust criterion, as suggested by our prior studies (Krasnov *et al.* 2013; Zikanov *et al.* 2014). To attain a statisticaly sustained (fully developed) state the simulations have typically run for the time from at least 100 to 1000 convetive time-units.

3. Results

3.1. *Low- and mid-range Re numbers*

We begin our discussion with the results of simulations at $Re = 500$ shown in Fig. 2a. This flow state has been obtained starting from a turbulent non-MHD duct at $Re = 1200$, as the smallest Re where turbulence can still exist. One interesting observation is that the turbulent energy drops by several orders of magnitude as the magnetic field is switched on. Basically, the magnetic field rapidly destroys turbulence so that remaining perturbations can be viewed as a residual noise. As a minimum is attained the residual fluctuations start to grow and finally evolve into another different unsteady regime. This behavior has also been found in other simulations initiated with non-MHD turbulent states.

Here we can clearly observe inherently small vortical structures located within the side wall region (Fig. 2a). The vortices exhibit anisotropy in the vertical z-direction, especially pronounced close to the Hartmann walls, as illustrated by the isosurfaces of λ_2-criterion. According to Jeong & Hussein (1995), negative regions of λ_2 identify coherent vortical structures (λ_2 is the 2^{nd} eigenvalue of the tensor $S_{ik}S_{kj} + \Omega_{ik}\Omega_{kj}$, where S_{ij} and Ω_{ij} are the rate of strain and vorticity tensors). The structures are comprised of clockwise vortices (CW, thinner ones at the side walls) and counter clockwise rotating vortices (CCW, thicker ones closer to the core). Both CW and CCW vortices are organized in a slightly staggered arrangement. These are the so-called TW vortices, first discovered by Ting and Walker (Ting *et al.* 1991). They appear at low-Re range and are viewed as the 1^{st} unstable solution of Hunt's flow. The TW vortices are very weak, e.g., for this case their kinetic energy is about 0.033% of the total kinetic energy of the flow (see Table 1), so hardly producing any visible impact on the integral flow charachteristics, such as the wall stresses τ_w or the total friction coefficient C_f.

Further increase of Re reveals an interesting and rather unexpected behavior of the flow. Namely, using this state as the initial condition and increasing Re to 1000, we have observed that TW vortices very quickly and nearly completely disappear during the initial phase of simulation. However, after about a hundred of convective units of temporal evolution, a new type of vortical structrures is developed. These new instabilities are similar to TW vortices, also arising at the side walls, but they are much larger, both in

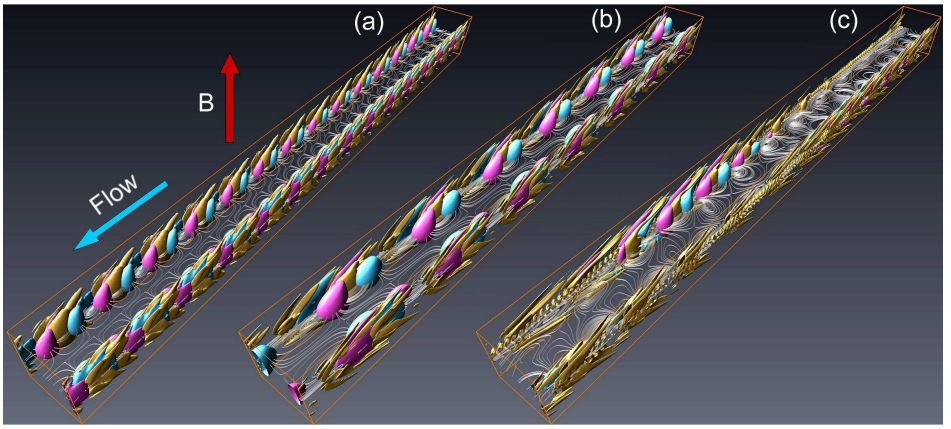

FIGURE 2. Instantaneous snapshots of flow states at $Re = 500$ (a), 1000 (b) and 1400 (c). Shown are isosurfaces of the second eigenvalue λ_2 of tensor $S_{ik}S_{kj} + \Omega_{ik}\Omega_{kj}$ (gold) and two isosurfaces of the spanwise velocity component u_y – positive (pink) and negative (cyan) of the same magnitude.

size and kinetic energy (about 0.1% of the total kinetic energy) and tend to dominate about 50...60% of the fluid domain (Fig. 2b). This particular behavior is observed in the range $1000 \leqslant Re \leqslant 1300$, where these big vortical strucuture have also been repeatedly reproduced in simulations initiated by non-MHD turbulent states. From the last two columns in Table 1 it appears that these vortices may be qualified as streaks.

Increasing Re to 1400, we again observe another different flow regime. New structures develop in the form of additional small-scale CW and CCW rotating vortices, which are located within the large instabilities previously observed at $1000 \leqslant Re \leqslant 1300$, which evolve in this case too. There are quite a few remarkable features concerning these structures. On the initial inspection, they are very small in size and elongated in the vertical z-direction, as demonstrated in Fig. 2c and in Table 1. The shape resembles that of "pike-teeth", which are settled in a staggered arrangement in respect to the mid-plane symmetry $z = 0$. Further analysis shows that the kinetic energy of these new structures is about two times smaller than the previous instabilities at $Re \leqslant 1300$, contributing 0.05% of the total kinetic energy of the flow. However, the specific distribution of the kinetic energy over fluctuating velocity components changes. Albeit the streamwise component is still dominating, the energy associated with the vertical component increases by a factor of 2, thus producing stronger anisotropy in the vertical direction. Basically, the "pike-teeth" can be viewed as rather strong (in amplitude) and short (in the vertical length) quasi-$2D$ modes. Once these structures have developed, they remain in the flow throughout the simulation. At higher Re (up to 1550) they develop more rapidly, stretching in the vertical direction, and demonstrate an oscillating pattern along the side walls.

To check the validity of the results we have conducted additional verifications. First, it has been found that these structures also arise if the simulation is initiated with turbulent duct flow state. Secondly, to make sure these structures were not a numerical artifact due to an insufficient grid, we have also performed simulations at even higher resolution of 2048×384^2 points and found them to appear again.

The "pike-teeth" have been observed in a narrow range $1400 \leqslant Re \leqslant 1550$, beyond which they are followed by another type of instability – jet detachments, discussed in the next section. Therefore, given the narrow range of Re and the gradually increasing level of kinetic energy vs. Re, it seems feasible to assume that the "pike-teeth" may serve a nuclei preceeding the detachments.

Re	q/Q_{tot}	q_t/Q_{tot}	q_y/q	q_z/q
500	0.033%	0.0081%	11.0%	13.5%
1000	0.10%	0.0125%	4.0%	8.5%
1400	0.05%	0.0110%	4.0%	18.0%
2000	10.0%	2.7%	19.0%	8.0%
5000	3.5%	1.5%	17.0%	26.0%

TABLE 1. TKE of velocity perturbations, shown in respect to the total kinetic energy of the flow Q_{tot} and as distribution over different componets of the fluctuating velocity. Listed are the TKE of all perturbations $q = \langle u_x^2 + u_y^2 + u_z^2 \rangle$ and the transverse part $q_t = q_y + q_z$, where $q_y = \langle u_y^2 \rangle$ and $q_z = \langle u_z^2 \rangle$. The brackets $\langle\rangle$ stand for volume averaging.

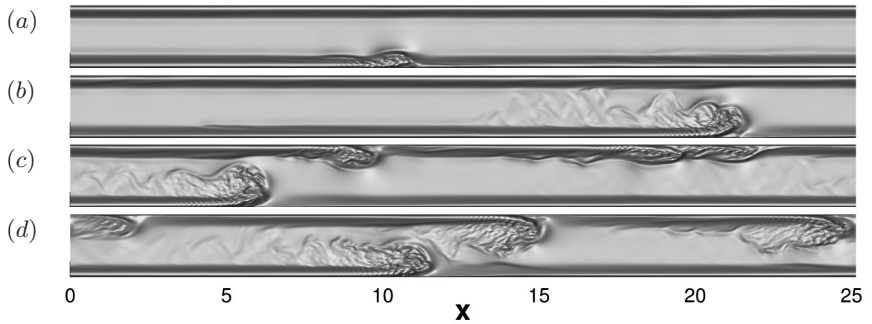

FIGURE 3. Temporal evolution of jet detachments at $Re = 1630$ and $Ha = 100$. Streamwise velocity u is shown in the (x, y)-mid-plane at $z = 0$, corresponding to four phases of evolution, beginning from a single event on one side-wall to the fully developed unsteady behavior (from top to bottom). Flow direction is from left to right, magnetic field vector is perpendicular to the (x, y)-plane.

3.2. *Jet detachments and transition to turbulence*

Upon further increase of Re upto 1630, we observe that the flow exhibits another time-dependent regime – partial jet detachments. The temporal evolution and settlement of this flow regime is shown in Fig. 3 with four phases, corresponding to the different times of flow evolution. One can see that in the beginning a very small nuclei of instability – a localized spot – appears at one side wall of the duct (a). As the time evolves, this spot grows in size and attains kinetic energy from the mean flow until the side jet visibly detaches from the wall (b). Soon after, the detached structure interacts with the opposite side wall, thus, producing a series of small disturbances also (c), which rapidly evolve into similar-sized instabilities. Consequently, both walls become populated with detached structures (Fig. 3d).

The nature of jet detachments can be understood more thoroughly from the analysis of vortex patterns formed at the side walls, as shown in Fig. 4 for $Re = 2000...5000$. The plot at $Re = 2000$ (Fig. 4a) demonstrates small CW rotating vortices, housed at the inner (near wall) region of the domain of the high velocity jet. They are a result of high shearing effects within the inner region of the duct. Simultaneously, CCW vortices are formed between the outer region of the velocity jet and the core flow. Initially, at $Re \leqslant 1600$, the small CCW vortices remain stable travelling in the streamwise direction along with the bulk of the flow. At some point the CCW vortices develop both in size and intensity and have a retarding effect on the velocity jet in the outer region. Eventually the CCW vortices have developed sufficiently enough to dramatically alter the flow regime and lift the jet away from the side wall in the y-direction, thus, the first jet detachment occurs.

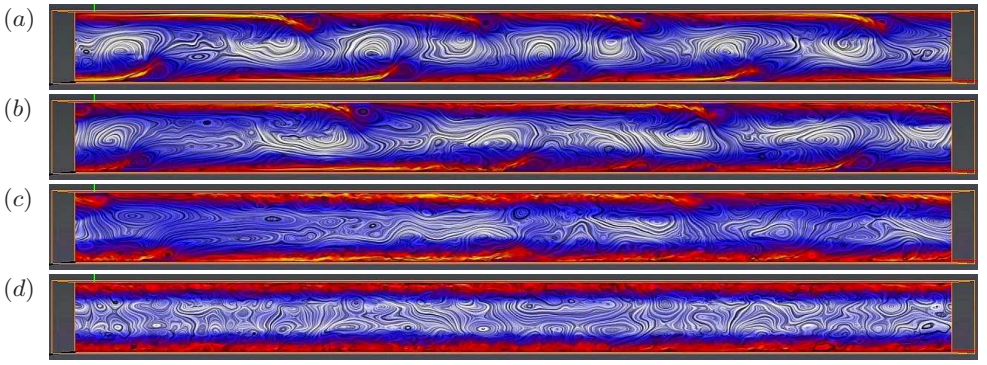

FIGURE 4. Transition of states with jet detachmens towards fully tubulent side-wall jets shown for $Re = 2000$ (a), 3000 (b), 4000 (c) and 5000 (d). Instantaneous vortical patterns in the (x, y)-mid-plane are visualized by the streamlines of fluctuating velocity field $\boldsymbol{v}$ in the (x, y)-mid-plane. Color gradient is highlighted by the magnitude of full-scale streamwise velocity component U_x. Flow direction is from left to right, magnetic field vector is perpendicular to the (x, y)-plane.

Once jet detachment has occurred, its evolution pushes the large CCW vortex through the core flow and hits the opposite wall. Here it interacts with CCW vortices on the opposite wall, thus generating one more detachment. We notice that the phenomenon of jet detachments is not entirely new, it has been observed in hydrodynamic flows (Bajura & Catalano 1974).

Further analysis has been conducted to address the dynamics of jet detachments and to explore the evolution towards even higher Re. We have performed a series of additional simulations and found that a staggered arrangement of partial jet detachments, as in Kinet *et al.* (2009), seems to be the preferred pattern. At the same time, the number of structures detached from the side walls is rather ambiguous: not only may it depend of the initial conditions, but also may change during the simulation. In some cases, we have observed non-symmetric flow states with only one wall populated by the spots, whereas the opposite wall remained unaffected for an extended period, sometimes more than a hundred of convetive time units. The evolution at increasing Re (Fig. 4*b*, *c*) indicate that the jet detachments gradually lose their characteristic form and develop small-scale structures in their trailing tail. It is clearly evident that already at $Re = 4000$ the side jets have become almost turbulent, albeit rare remains of the detachments are still present. Finally, at $Re = 5000$ (Fig. 4*d*) the side wall regions become eintirely turbulent. A remarkable feature is the stabilization of the core flow as Re increases, which is particularly well observed at $Re \geqslant 5000$. Here the core flow carries weak quasi-$2D$ vortical structures and remains essentially uninvolved in an unsteady motion.

3.3. *Hysteresis*

In the previous sections we have demonstrated various flow regimes and, correspondingly, the appearance of different types of instabilities, as Re is increased as a single shot or, alternatively, as the magnetic field is instantly switched on. Here we shall study the flow evolution with yet another approach – changing Re in smaller steps of 100, applying either increments (moving up) or decrements (moving down the Re axis). For the incremental simulations, the initial state at $Re = 500$ and $Ha = 100$, populated with weak TW vortices, have been used. Intrinsically, during the incremental runs we have not found any remarkable differences to the previously obtained results (sections 3.1 and 3.2). All flow regimes and the corresponding types of instabilities have been identified at essentially the same ranges of Re, e.g., streaks at $Re = 1000...1100$, "pike teeth" at

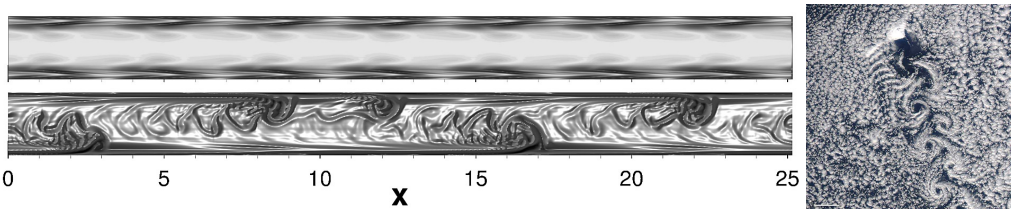

FIGURE 5. Instantaneous snapshots of flow fields at $Re = 1000$ shown for incremental (left-top) and decremental (left-bottom) simulations. The flow patterns are visualized by the vertical vorticity component ω_z in the (x, y)-mid-plane. On the right plot there is a photograph of cloud formation around Jan Mayen Island, Greenland (courtesy of NASA).

1400, beginning of jet detachments at 1600...1700 and turbulization of the side jets at $Re > 4000$.

The situation changes in reverse simulations "down the hill", starting from a state of $Re = 10000$ with turbulent side jets. The initial and relatively long part between $10000 \geqslant Re \geqslant 2000$ demonstrates a mirroring of flow regimes vs. the incremental runs, i.e. gradual transition from turbulence to jet detachments. However, a continued further decrease of Re reveals no appearance of other intability types, identified in the incremental simulatons. Instead, unstable flow regimes with jet detachments continue until $Re = 200$, albeit the kinetic energy of perturbations gradually decreases. This behavior demonstrates the phenomenon of hysteresis or, broadly speaking, multiplicity of possible states and solutions, which appear depending of the particular route. A remarkable feature is that hysteresis has been observed in a very broad range $200 \leqslant Re \leqslant 2000$, inherently in the parameter space varying by one order of magnitude. Similar hysteresis effects were also observed in the prior study (Kinet *et al.* 2009) of duct flow with finite wall conductivity. However, the range of Re with multiple states was far more narrow. An example of such a hysteresis is shown in Fig. 5 for two different flow states at the same $Re = 1000$. We can see both the pattern typical for CW and CCW vortices (Fig. 5, top-left) and jet detachments (Fig. 5, bottom-left) obtained in, correspondingly, incremental and decremental simulations.

This figure also serves the purpose of demonstrating yet another interesting effect – the phenomenon of vortex shedding in the form similar to that of a von Karman street. We have found that this effect is predominantly expressed at low-Re range. The motion of detached structures through the domain generates a vortex shedding in their downwind, thus, producing patterns typical for flows past a solid obstacle. To further highlight this similarity and also to illustrate this effect being a common feature for many hydrodynamic systems, we provide an example of completely different scale (Fig. 5, right). This is a photograph of atmospheric cloud formation around Jan Mayen Island, Greenland (Earth Observatory, NASA (2012)), one can clearly see the essentially same von Karmann street. Even the ribs at the left side are nearly identical to near-wall ones in our problem.

4. Summary

The instability of Hunt's flow with ideally conducting Hartmann walls and insulating side walls has been studied numerically at a fixed $Ha = 100$, which corresponds to moderate magnetic fields, and a broad range of Re varying from 200 to 10000. Upon increasing Re several unsteady flow regimes have been identified, including the TW vortices (low $Re < 1000$), partial jet detachments (mid-range of $Re \geqslant 1630$) and transition to fully developed turbulence in the side-wall jets (upper range of $Re \geqslant 5000$). In addition, two new instabilies are discovered: large streaks ($1000 < Re < 1400$) and

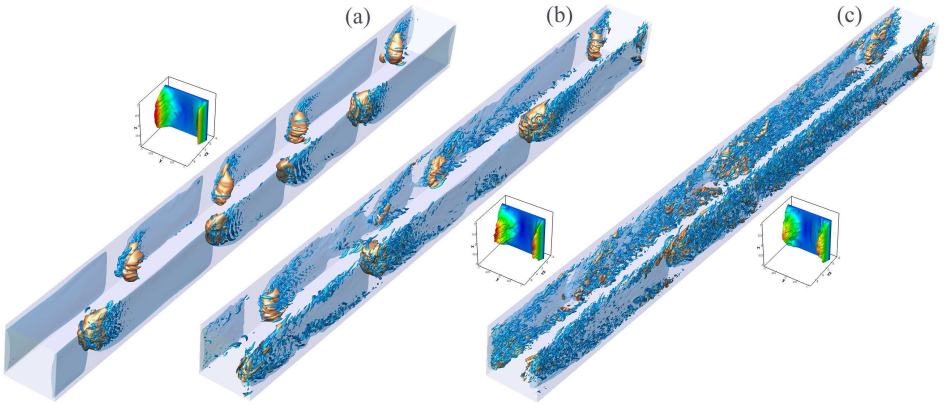

FIGURE 6. Evolution of jet detachments versus Re, instantaneous snapshots of flow fields are visualized at $Re = 2000$ (a), 3000 (b) and 4000 (c). Shown are the isosurfaces of full-scale streamwise velocity u_x at the side walls (light blue), TKE of transverse velocity fluctuations $u_y^2 + u_z^2$ (gold) and λ_2 criterion (cyan). The inserts show velocity profiles in the (y, z)-section at $x = L_x/2$.

very small, tightly localized at the side walls, vertical "pike-teeth" structures ($1400 < Re < 1550$). The results of our simulations suggest that these structures can be regarded as "sub-instabilities", connecting the other, major types of unstable solutions. Indeed, these two new regimes are found in rather narrow ranges of Re, being quickly followed by, or proceeded by another persistent unsteady solution.

Our simulations also suggest another view on the instability of Hunt's flow. Namely, given the extremly low amplitude of TW vortices observed at low-Re, one may speculate that the actual transition to the truly unsteady flow states should be viewed beginning from the appearance of jet detachments. By adopting this point of view, we can see the laminar-turbulent transition in Hunt's flow is not a unique feature, but is rather similar to other MHD and non-MHD shear flows. Indeed, approaching the critical range of $Re \approx 1600$, detachments first appear in the form of sporadic events, i.e. essentially isolated spots residing in the side wall layers. As Re increases, the side walls become increasingly populated with such spots, which keep developing small-scale fluctuations, until the entire extent of the side wall is involved into fully turbulent motion, as demonstrated in Fig. 6. Very similar flow dynamics with puffs bordering laminar and turbulent regimes is well known for many other shear flows, in particular for MHD duct and pipe flows with insulating walls (Krasnov *et al.* 2013; Zikanov *et al.* 2014), where the puffs are localized at the side walls. Even the non-symmetry of pattern arrangements at the opposite side walls is observed too. The clearly novel feature of Hunt's flow instability is that these transient states are observed in a much broader range of Re numbers, distinguishing it apart from other shear flows. The same observation also applies for multiple states and hysteresis, found in an extremely broad range $2000 \geqslant Re \geqslant 200$.

At the early stages of jet detachments, the vortical structure detaching from the wall can also produce the effect very similar to that of an obstacle, which is observed seen since the velocity of the core flow is much smaller than in the jet. As a result, the phenomenon of vortex shedding typical to a von Karman street may form.

Another distinct feature we have observed is the non-monotonic behavior of the core flow versus increasing Re number: essentially unperturbed core flow at low-Re regimes (TW vortices), evolution into a strong unsteady motion at moderate Re (jet detachments) and approaching amost unperturbed state, populated with weak quasi-2D structures at high Re (turbulent side-wall jets). This particular behavior of the core flow has practical

implications. Namely, the most unsteady regimes at intermediate values of Re seem the most preferred ones to intensify flow mixing and, correspondingly, enhance heat transfer, which is the ultimate purpose of fusion blankets.

The work of Lee Braiden was in part carried out within the framework of the EUROfusion Consortium and has received funding from the Euratom research and training programme 2014-2018 under grant agreement No 633053. The views and opinions expressed herein do not necessarily reflect those of the European Commission.

Lee Braiden is greatful to the Engineering and Physical Sciences Research Council and Culham Centre for Fusion Energy (UK) for the award of an Industrial CASE PhD studentship. DK gratefully acknowledges financial support by the German Helmholtz Association in the frame of the Helmholtz-Alliance LIMTECH. Computer resources were provided by the computing centers of Coventry University, Forschungszentrum Jülich (NIC) and TU Ilmenau.

REFERENCES

Bajura, R. A. & Catalano, M. R. 1974 Transition in a two-dimensional plane wall jet. *J. Fluid Mech.* **70**, 773–799.

Bühler 2007 Liquid metal magnetohydrodynamics for fusion blankets. In *Magnetohydrodynamics - Historical Evolution and Trends* (ed. R. Moreau S. Molokov & H. K. Moffatt), pp. 171–194. Springer.

Earth Observatory, NASA 2012 The Moderate Resolution Imaging Spectroradiometer (MODIS) instrument on NASA's Aqua satellite captured the image on April 4, 2012. http://earthobservatory.nasa.gov/NaturalHazards/view.php?id=77654.

Hunt, J. C. R. 1965 Magnetohydrodynamic flow in rectangular ducts. *J. Fluid Mech.* **21**, 577–590.

Jeong, J. & Hussein, F. 1995 On the identification of a vortex. *J. Fluid Mech.* **285** (1), 69–94.

Kinet, M., Knaepen, B. & Molokov, S. 2009 Instabilities and Transition in Magnetohydrodynamic Flows in Ducts with Electrically Conducting Walls. *Phys. Rev. Lett.* **103**, 154501.

Knaepen, B., Kinet, M. & Molokov, S. 2009 Instabilities of side-layer jets in magnetohydrodynamic duct flows. In *Proc.* 6^{th} *Int. Conf. on Electromagnetic Processing of Materials*, pp. 45–48. Dresden, Germany.

Krasnov, D., Thess, A., Boeck, T., Zhao, Y. & Zikanov, O. 2013 Patterned turbulence in liquid metal flow: Computational reconstruction of the Hartmann experiment. *Phys. Rev. Lett.* **110**, 084501.

Krasnov, D., Zikanov, O. & Boeck, T. 2011 Comparative study of finite difference approaches to simulation of magnetohydrodynamic turbulence at low magnetic Reynolds number. *Comp. Fluids* **50**, 46–59.

Lielausis, O. 1975 Liquid-metal magnetohydrodynamics. *Atomic Energy Review* **13**, 527–581.

Müller, U. & Bühler, L. 2001 *Magnetohydrodynamics in channels and containers*. Springer, Berlin.

Priede, J., Aleksandrova, S. & Molokov, S. 2010 Linear stability of Hunt's flow. *J. Fluid Mech.* **649**, 115–134.

Reed, C. B. & Picologlou, B. F. 1989 Side wall flow instabilities in liquid metal mhd flow under blanket relevant conditions. *Fusion Techn.* **15**, 705–715.

Roberts, P. H. 1967 *An introduction to Magnetohydrodynamics*. New York: Longmans, Green.

Schmid, P. J. & Henningson, D. S 2001 *Stability and Transition in Shear Flows*. Springer, Berlin.

Ting, A. L., Walker, J. S., Moon, T. J., Reed, C. B. & Picologlou, B. F. 1991 Linear stability analysis for high-velocity boundary layers in liquid-metal magnetohydrodynamic flows. *Int. J. Engng. Sci.* **29** (8), 939–948.

Zikanov, O., Krasnov, D., Li, Y., Boeck, T. & Thess, A. 2014 Patterned turbulence in spatially evolving magnetohydrodynamic tube flows. *Theor. Comp. Fluid Dyn.* **28** (3), 319–334.